Ranging in IR-UWB Networks : Survey and Modelling of Synchronization Error

Robin Scheibler

under supervision of
Ruben Merz
Prof. J.-Y. Le Boudec

LCA2, EPFL

June 30, 2008

Abstract

This work can be divided into two distinct parts. The first one is a survey of the state-of-the-art in ranging and localization techniques applied to sensor networks. This is a preliminary study for the implementation of a distributed ranging protocol for Impulse Radio - Ultra Wide Band (IR-UWB) network. The type of measurement, practical measure scenarios as well as algorithms for ranging are revised. A performance comparison of Least-Squares and Maximum Likelihood localization was done to get an understanding of the behavior and limitations of classical techniques when the measurement noise is non-Gaussian. Techniques of interest for UWB sensor networks are identified. The second part is the modelling of the synchronization error for a 802.15.4a energy-detector receiver. Synchronization is one of the main source of error when doing ranging using UWB. Nevertheless, most studies model it as Gaussian noise on the distance measurement. However this is far from what happens on practical UWB channels and non-Gaussian noise leads to serious degradation of performance of localization algorithms. It is therefore vital to get a good understanding of the synchronization error to help design efficient ranging schemes.

Contents

1 Survey of Localization Techniques in Sensor Networks

1.1 Types of Measurements

The problem of localization is essentially a geometrical problem. As such, there is two types of measurements that can be used to solve it : angles and distances. The main methods to take those measurements using a radio link are summarized here. For more detailed surveys, see [1, 2, 3].

Direction Of Arrival (DOA)   The angle measurements are usually carried out as DOA estimation (sometimes also called Angle Of Arrival). This technique is related to beamforming and thus requires an antenna array. However, an antenna array is typically not available on sensors as they must be as small and cheap as possible.

Received Signal Strength (RSS)   RSS is defined as the received signal power. It is used to estimate the distance of the source of the signal. However, on a typical wireless link the received power behaves in a particularly unpredictable fashion. That's why it is preferable to use more reliable techniques such as the ones that will be described now.

Time Of Arrival (TOA)   This technique uses the knowledge of the transmission and arrival times, t_t and t_a, to compute the propagation time. Then, the distance can be roughly estimated as :

$$r = t_{prop} \times c = (t_a - t_t) \times c, \tag{1}$$

where t_{prop} is the propagation time and c the speed of light. As a rule of thumb, 1 ns translates roughly to 30 cm. In the case of one-way transmission, synchronization of the clocks of the transmitter and receiver is required. To avoid this, two-way transmissions can be used (cf. 1.2.2 for more details). But, in this case the processing time t_{proc} at the target node must be taken into account and we have :

$$t_{prop} = \frac{t_a - t_t - t_{proc}}{2}. \tag{2}$$

The TOA method is particularly suitable for UWB communication as it can achieve a very fine time resolution.

Time Difference Of Arrival (TDOA) Instead of trying to estimate the distance between the target and a reference node, TDOA attempts to estimate the difference of the distance between the target and a first reference node and the distance between the target and a second reference node. Supposing we have N reference nodes n_1 to n_N that want to localize a target node T, we don't use the propagation time, but instead the difference of the propagation times to two reference nodes n_i and n_j :

$$\Delta t_{ij} = (t_a^i - t_t) - (t_a^j - t_t) = t_a^i - t_a^j. \tag{3}$$

Therefore the difference of distances is :

$$\Delta r_{ij} = r_i - r_j = (t_a^i - t_t) \times c - (t_a^j - t_t) \times c = (t_a^i - t_a^j) \times c \tag{4}$$

Therefore, the clock of the target node need not be synchronized with the reference nodes, but the reference nodes have to be synchronized with each others. This requirement can however be overcome by using differential TDOA (dTDOA) as described in [4].

This method as well is very suitable for UWB networks as it also implies timing measurements.

1.2   Practical Distance Measurements Scenarios

Before running any localization algorithm, we need a protocol that allows the reference nodes to make the geometrical measurements in an efficient way. From the different possible measurements presented in the last section, we only retain TOA and TDOA as they don't require any specialized hardware on top of the UWB radio transceiver and give the best performance. DOA requires at least two antennas while RSS gives at most poor performance. The latter could eventually be used in addition to TOA or TDOA to refine the measurement. However, this is left for further work.

In many cases, synchronization of the clocks of the nodes reduce the communication overhead when doing the measurements (e.g. one-way against two-way TOA). However maintaining clock synchronization in a sensor network might be very costly or even not feasible at all. Therefore, we analyze scenarios with full, partial and no clock synchronization to get an idea of the overhead introduced by the lack of synchronization.

The processing and exchange of measurements between the reference nodes needed for the localization are not addressed here.
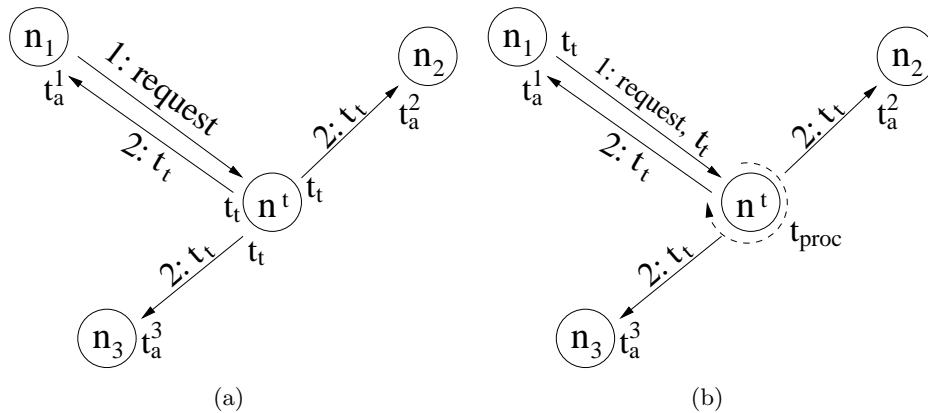
Figure 1: Message exchange scenarios for the measurements of TOA with (a) full synchronization (b) partial synchronization.

1.2.1 Scenario considered and assumptions

We assume the nodes lie on a 2D plane. There is N quasi static reference nodes n_1 to n_N who already know their position with a high degree of accuracy. This is justified by the fact that if the nodes don't move frequently, they have plenty of time to perform averaging on several measurements and get a good estimate of their relative positions. Those reference nodes try to locate a relatively slow moving target node n^t. The slow moving assumption only ensures that we don't have severe time constraint while performing localization of n^t.

Regarding synchronizations of the clock of the nodes, we study three different situations :

- The clocks of all the nodes are synchronized (full synchronization).

- Only the clocks of the reference nodes are synchronized (partial synchronization).

- All the clocks are asynchronous (no synchronization).

The ways synchronization can be achieved are described in section 1.2.4.

1.2.2 TOA

Full Synchronization In case of TOA and full synchronization, the following scenario, illustrated in Fig. 1 can be followed :

4
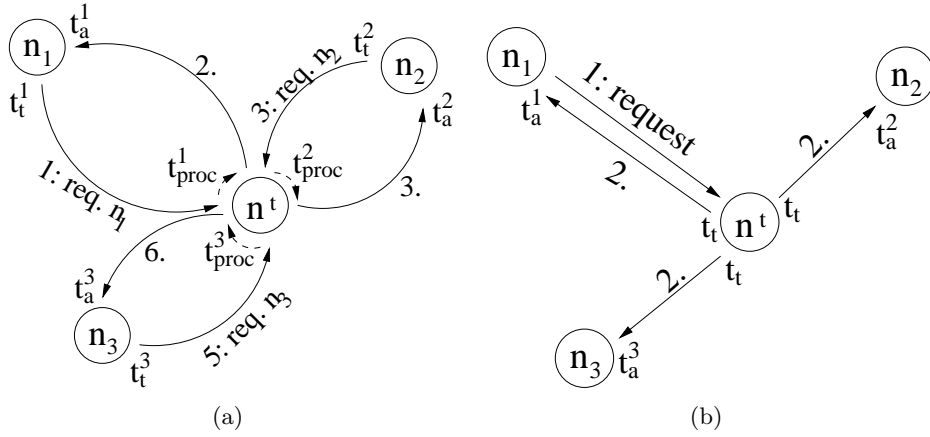
Figure 2: Message exchange scenarios for the measurements of (a) asynchronous TOA (b) TDOA (partial synchronization).

1. One of the reference nodes sends a message to n^t to request localization.

2. Upon reception of the request, n^t broadcast a message containing a timestamp of t_t, the transmission time.

3. When receiving this message, the reference nodes can subtract the arrival time t_a to t_t and get the propagation time.

4. Then, the reference nodes cooperate to localize n^t using the propagation time information.

Partial Synchronization   The following scenario is illustrated in Fig. 1 :

1. One of the reference nodes (i.e. n_1) sends a message to the target node to request localization. In this message, n_1 inserts t_t, the time of the transmission of the message.

2. Upon reception, the target node broadcasts a message containing t_t to all reference nodes.

3. The the arrival times at the reference nodes n_1 to n_N, respectively denoted by t_a^1 to t_a^N are recorded by the reference nodes.

4. Then, the reference nodes cooperate to localize n^t.

5

In this case, we obtain the propagation time from n_1 to n^t added to the propagation from n^t to n_i (plus some processing time t_{proc} at n^t). This leads to the following sets of measurements :

$$
\begin{aligned}
m_1 &= t_a^1 - t_t = 2t_{prop}^1 + t_{proc} \\
m_2 &= t_a^2 - t_t = t_{prop}^1 + t_{proc} + t_{prop}^2 \\
&\vdots \\
m_N &= t_a^N - t_t = t_{prop}^1 + t_{proc} + t_{prop}^N
\end{aligned}
$$

Then, knowing t_{proc} we can recover the propagation times :

$$
t_{prop}^i = m_i - \frac{m_1 + t_{proc}}{2} \quad , \quad i = 1, \ldots, N \tag{5}
$$

No Synchronization   In this case, every reference node need to perform a two-way message exchange with n^t Fig. 2 :

1. n_i sends a message to n^t to request a distance measurement. n_i records the time t_t^i it sent this message.

2. n^t replies to n_i. This adds a delay t_{proc}^i to the round-trip time.

3. Using the time of arrival t_a^i, n_i can compute the propagation time as :

$$
t_{prop}^i = \frac{t_a^i - t_t^i - t_{proc}^i}{2} \tag{6}
$$

4. This is repeated by every reference node, until all of them have a measurement.

5. The reference nodes cooperate to localize n^t.

1.2.3   TDOA

TDOA requires only the synchronization of the reference nodes. Therefore, full synchronization does not bring any further advantage than partial synchronization and is not considered. As TDOA cannot be applied to the asynchronous case, it is not considered as well. However, there exists asynchronous schemes that use differential TDOA that should be studied as well, for example [4].

Partial Synchronization   The following scenario is illustrated in Fig. 2:

1. One of the reference nodes sends a message to n^t to request localization.

2. Upon reception of the request, n^t broadcasts a message to the reference nodes.

3. The reference nodes will record the time of arrival t_a^1 to t_a^N of this message.

4. Then, this information is exchanged between the different reference nodes and the TDOA measurements as described in section 1.1 can be used to localize the target.

1.2.4   Clock Synchronization

There is basically two alternatives to synchronize the clocks of the nodes :

1. Terrestrial Radio Clock Synchronization : In many countries an atomic clock time is broadcast using radio waves. It is a straightforward and cheap way of synchronizing sensors. The hardware requirement is also quite low as it is implemented in many very low-cost alarm clocks widely available on the market. However, the precision of such a system should be verified.

2. Clock Synchronization Algorithms : Many such algorithms have been proposed. For a survey of those, see [5]. However, the synchronization obtained is only of the order of ten millisecond which is by far not sufficient for ranging applications.

To give an idea of the precision we need, consider that 1 nanosecond and 1 millisecond are roughly equivalent to respectively 30 centimeters and 300 meters. Therefore for a precision in the order of the meter we need less than 3 ns and in the order of ten meters we need less than 30 ns.

1.2.5   Trade-off between synchronization and overhead

Synchronization of the nodes' clock reduces considerably the overhead as it result in a single broadcast from the target node. However, the precision of synchronization algorithms is not sufficient for ranging applications. On top of that, such algorithms would introduce overhead superior to the gain due to synchronization. The only alternative would be synchronization from an

external clock, like terrestrial radio clock. However, the cost in hardware and the precision of such a system is not clear and should be studied.

1.2.6   Sources of errors in TOA and TDOA

- Synchronization errors at the receiver directly affect both TOA and TDOA. The distribution of the synchronization error with an energy-detection receiver for 802.15.4a is studied in Section 2.

- Processing time t_{proc} when using schemes that require more than a single message to be exchanged.

- Clocks synchronization errors when using synchronous schemes.

- Clock drift and jitter.

- Circuitry induced delays.

1.3   Localization of Isolated Nodes

Once we have taken those measurements, we still need to compute the co-ordinates of n^t. When using TOA, the problem is known as trilateration. It boils down to finding the intersection of N circles centered on n_1 to n_N with radius r_1 to r_N, where $r_i = t_{prop}^i \times c$. In the case of TDOA, we speak of multilateration and the problem is to find the intersection of hyperbolas [6]. Here, we concentrate on TOA localization but similar methods can be used with TDOA.

First, the basic trilateration with no measurement error is recalled. Then, two estimation methods used to mitigate measurement errors are presented : Least-Squares and Maximum Likelihood estimation.

1.3.1   Trilateration

When there is no measurement error, three reference nodes are sufficient to localize n^t on the plane. Without loss of generality we assume n_1 to be at the origin, n_2 to lie on the x-axis with coordinate $(a; 0)$ and n_3 to have coordinate $(b; c)$ as shown in Fig. 3. Then the solution of the following system of circle equations gives the position $(x; y)$ of n^t :

$$\begin{cases} x^2 & + & y^2 & = & r_1^2 & (i) \\ (x-a)^2 & + & y^2 & = & r_2^2 & (ii) \\ (x-b)^2 & + & (y-c)^2 & = & r_3^2 & (iii) \end{cases} \tag{7}$$
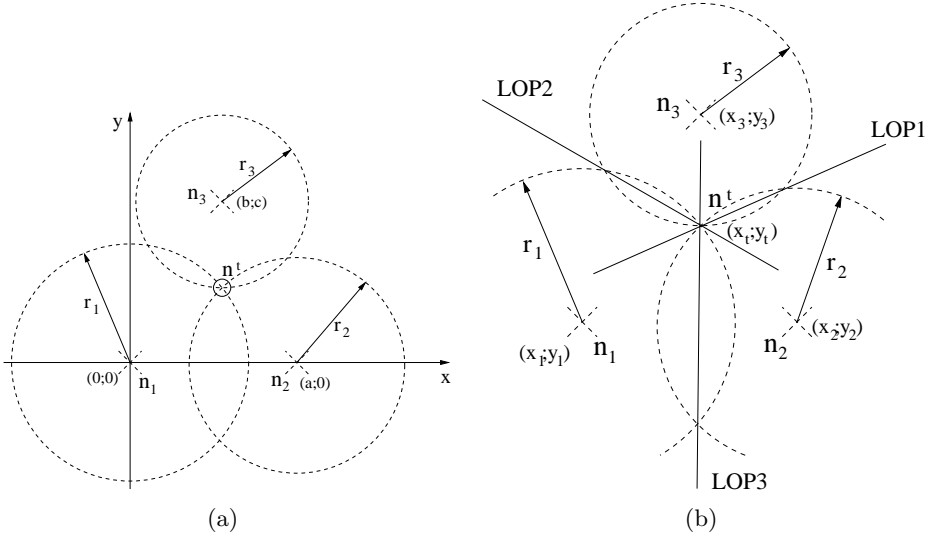
Figure 3: (a) Trilateration (b) Least-Squares Estimation of the intersection of the Lines Of Positons (LOP)

By replacing $y^2 = r_1^2 - x^2$ in (ii) and $x^2 = r_1^2 - y^2$ in (iii) we obtain :

$$\begin{cases} x &= \frac{a^2 + r_1^2 - r_2^2}{2a} \\ y &= \frac{b^2 + c^2 + r_1^2 - r_3^2}{2c} - \frac{b}{c}x \end{cases} \qquad (8)$$

However, when measurement errors are present, all the circles will not intersect at the same point anymore. Therefore we need to use some more advanced technique to find the best estimate for the position of x^t according to some error function.

1.3.2 Least-Squares Estimation (LSE)

When measurement noise is present, a way of mitigating the localization error is to use a least-squares strategy [7]. Consider the N reference nodes n_1 to n_N with respective coordinates $(x_1; y_1)$ to $(x_N; y_N)$ and the target node n^t with unknown coordinates $(x_t; y_t)$. Then, the distance between n_i and n^t can be expressed as :

$$r_i = \sqrt{(x_i - x_t)^2 - (y_i - y_t)^2} \qquad (9)$$

9

Now, by squaring and subtracting Eq. (9) with respect to nodes n_k and n_l, $k \neq l$, we obtain :

$$r_k^2 - r_l^2 = (x_k - x_t)^2 - (y_k - y_t)^2 - (x_l - x_t)^2 + (y_l - y_t)^2 \qquad (10)$$

By rearranging the terms in this equation we get:

$$(x_k - x_l)x_t + (y_k - y_l)y_t = \frac{1}{2}(\|n_k\|^2 - \|n_l\|^2 + r_l^2 - r_k^2) \qquad (11)$$

where $\|n_i\|^2 = x_i^2 + y_i^2$, the squared norm of the vector position of n_i. Note that this equation is linear in the unknown x_t and y_t. This actually define a straight line, called Line Of Position (LOP), going through the intersections of the two circles centered on n_k and n_l as shown in Fig. 3. Without noise, all those LOP intersect at the position of n^t. However, when r_i is replaced by its noisy TOA measurement $\hat{r}_i$ the lines don't intersect anymore and we get the following equation:

$$(x_k - x_l)x_t + (y_k - y_l)y_t = \frac{1}{2}(\|n_k\|^2 - \|n_l\|^2 + \hat{r}_l^2 - \hat{r}_k^2). \qquad (12)$$

But with N reference nodes, we get at most $N(N-1)/2$ such linear equations. Therefore, we can find the least-squares estimate of the coordinates of n^t. Let's first define :

$$A = \begin{bmatrix} (x_2 - x_1) & (y_2 - y_1) \\ (x_3 - x_1) & (y_3 - y_1) \\ \vdots & \vdots \\ (x_N - x_1) & (y_N - y_1) \end{bmatrix}, \qquad (13)$$

and

$$b = \begin{bmatrix} \frac{1}{2}(\|n_2\|^2 - \|n_1\|^2 + \hat{r}_1^2 - \hat{r}_2^2) \\ \frac{1}{2}(\|n_3\|^2 - \|n_1\|^2 + \hat{r}_1^2 - \hat{r}_3^2) \\ \vdots \\ \frac{1}{2}(\|n_N\|^2 - \|n_1\|^2 + \hat{r}_1^2 - \hat{r}_N^2) \end{bmatrix}. \qquad (14)$$

Then, the LSE of $\boldsymbol{\theta} = [x_t, y_t]^T$ can be obtained as :

$$\hat{\boldsymbol{\theta}} = (A^T A)^{-1} A^T b \qquad (15)$$

Here, we only used the lines generated by the intersection of the circle centered in n_1 with the other circles, but in practice we could use all the straight lines generated by all pairs of circles.

10

This method has the advantage to be non-parametric and hence does not make any assumption on the distribution of the measurement error. However, the computational cost is proportional to $O(N^3)$ because of the matrix inversion. This complexity could be handled using a distributed approach as proposed in [8].

1.3.3 Maximum Likelihood Estimation (MLE)

The idea here is to make some assumptions on the distribution of the measurement error and derive the maximum likelihood estimator (MLE) of the coordinates of n^t. If the assumptions made are close enough to reality, the localization error might be reduced significantly compared to non-parametric method such as the Least-Squares estimation presented before. Such an MLE was derived for independent zero-mean Gaussian measurement errors in [9].

Keeping the same notation, we have N independent noisy TOA measurements :

$$t_{prop}^i = \frac{r_i}{c} + \epsilon_i \quad , \quad i = 1, \ldots, N \tag{16}$$

where $\epsilon_i \overset{iid}{\sim} \mathcal{N}(0, \sigma)$ and i is the index of the reference node. Then the probability density function (pdf) of $\boldsymbol{T} = [t_{prop}^1, \ldots, t_{prop}^N]^T$ given $\boldsymbol{\theta}$, the coordinates of n^t, is :

$$f(\boldsymbol{T}|\boldsymbol{\theta}) = (2\pi)^{-\frac{N}{2}} (det\boldsymbol{Q})^{-\frac{1}{2}} \exp\left(-\frac{J}{2}\right) \tag{17}$$

where

$$J = \left[\boldsymbol{T} - \frac{\boldsymbol{r}(\boldsymbol{\theta})}{c}\right]^T \boldsymbol{Q}^{-1} \left[\boldsymbol{T} - \frac{\boldsymbol{r}(\boldsymbol{\theta})}{c}\right] \tag{18}$$

with $\boldsymbol{Q} = diag(\sigma^2, \ldots, \sigma^2)$, the covariance matrix, and $\boldsymbol{r}(\boldsymbol{\theta}) = [r_1, \ldots, r_N]^T$, the vector of true distances. The MLE will be :

$$\hat{\boldsymbol{\theta}} = \arg\min_{\boldsymbol{\theta}}\{J\} \tag{19}$$

Setting the gradient of J to zero with respect to the two parameters x_t and y_t yields :

$$
\begin{aligned}
\frac{\partial}{\partial x_t} J(\boldsymbol{\theta}) &= \sum_{i=1}^{N} \frac{(r_i - t_{prop}^i c)(x_t - x_i)}{r_i} &= 0 \\
\frac{\partial}{\partial y_t} J(\boldsymbol{\theta}) &= \sum_{i=1}^{N} \frac{(r_i - t_{prop}^i c)(y_t - y_i)}{r_i} &= 0
\end{aligned}
\tag{20}
$$

Because $r_i = \sqrt{(x_i - x_t)^2 + (y_i - y_t)^2}$, those equations are non-linear in the unknowns and require the use of some iterative optimization algorithm such as gradient descent or Newton's method to find the minimum of $J(\boldsymbol{\theta})$.

1.3.4 Comparison of LSE and MLE

To evaluate the performance of LSE and MLE a small simulation on Matlab was set up. One target and N reference nodes are uniformly distributed on a 100 by 100 meters squared surface. The distance between the reference nodes and the target is computed and some noise is added to this distance. The LSE is implemented as presented above using all the $N(N-1)/2$ equations available. The MSE implementation uses the matlab function `fminsearch` to solve the optimization problem of Eq. (19).

The performance metric used is the Mean Error (ME) distance between the true and the calculated position. The SNR is defined in this case as the true-distance to measurement error power ratio. Both Gaussian and non-Gaussian measurement noise are studied. In the non-Gaussian case, a mixture of three Gaussian with a bias for positive values is used.

The results shown in Fig. 4 were obtained with 1000 repetitions for each point. The MLE outperforms the LSE when the noise is Gaussian. This is expected since the MLE models the noise as Gaussian. When the noise is not Gaussian, the MLE outperforms the LSE when the number of reference nodes is small but their performance is asymptotically identical. When the noise is not Gaussian, both the MLE and the LSE needs very high SNR to give an acceptable performance.

2 Modelling of Synchronization Error in 802.15.4a with an Energy-Detection receiver

A first step in the analysis of the performance of ranging with an energy-detection receiver for 802.15.4a is the analysis and modelling of the synchronization error which directly affects both TOA and TDOA. A good error model has multiple use in the design and performance evaluation of ranging algorithms. First of all, it allows to simulate the ranging without simulating the underlying physical layer that does the synchronization. Secondly it could be used to derive the MLE according to an error model closer to the reality. Indeed it was shown in section 1.3.4 how the performance drops when the error does not fit the model used to derive the MLE.
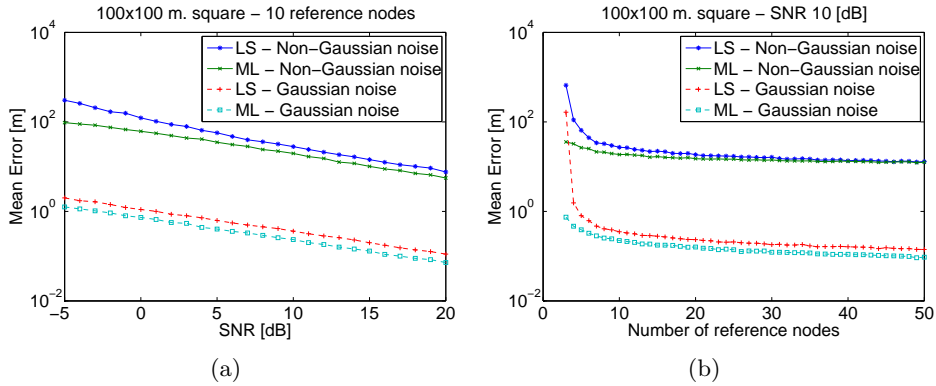
Figure 4: Performance comparison of Maximum Likelihood and Least-Squares Estimation of the position of the target node. (a) The Mean Error (ME) as a function of the SNR of the distance measurement with 10 reference nodes. (b) The ME as a function of the number of reference nodes for an SNR of 10 dB.

T_c	L	T_{int}	$Thld_{prob}$	G	N	M
2e-9	64	2e-9	0.9999	8	16	2

Table 1: Simulation parameters used to generate the dataset.

2.1 Experiment Conditions

The measurement of the synchronization error was done using the 802.15.4a energy-detection physical layer simulator developed by Ruben Merz and Manuel Flury at LCA2. The error is defined as the offset between the synchronization time and the true time of arrival. This offset is rounded to a precision of 0.1 ns. Simulation parameters are given in 1. At the end of the simulations, only successful synchronizations were kept. Indeed, when synchronization fails ranging is not possible. Mainly the single user case was considered. In a second time, simulations were also done with one interferer with power ten times superior to the user of interest. But in this case, only an histogram is shown. The statistical analysis is left for further work.
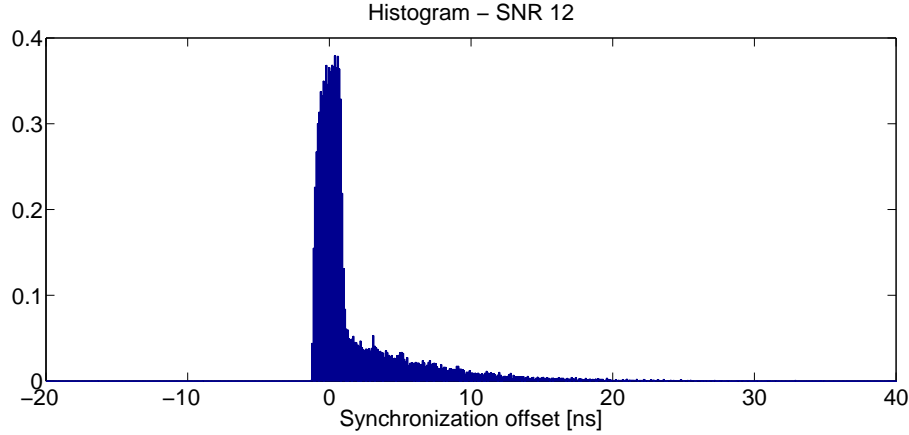
Figure 5: The histogram of the synchronization offset at an SNR of 12 dB.

2.2 Single User

To begin the analysis, it is useful to look at the histogram of the distribution of the synchronization error Fig. 5. We can see that there is roughly three parts that seems to follow distinct distributions. The first one that we'll call the nose contains all the samples smaller than some bound located around $\alpha \approx -1.5$ ns. Then there is a central part that will be called peak located around 0 ns, the correct synchronization point. The last part called the tail begins at about $\beta \approx 1.2$ ns. Therefore, the samples were separated in three groups : $S_{nose} = \{x|x \in [-32;\alpha[\}$, $S_{peak} = \{x|x \in [\alpha;\beta]\}$ and $S_{tail} = \{x|x \in]\beta;+\infty[\}$. The values of α and β were chosen manually by looking at the histograms. The hard limit at -32 ns comes from the back search algorithm implemented in the simulator. Then, the final distribution will look like :

$$f_{offset}(x) = \begin{cases} p_{nose}f_{nose}(x) & \text{if } x \in S_{nose} \\ p_{peak}f_{peak}(x) & \text{if } x \in S_{peak} \\ p_{tail}f_{tail}(x) & \text{if } x \in S_{tail} \end{cases} \quad (21)$$

where $p_{nose} = \mathbb{P}\{x \in S_{nose}\}$ is estimated as $|S_{nose}|/N$ and N is the total number of samples. p_{peak} and p_{tail} are defined similarly.

As the nose contains very few samples, it is difficult to characterize. It was compared with Quantile-Quantile (QQ) plot to a reverse truncated exponential (because of the hard limit). The QQ plot in Fig. 6 seems to show a fairly straight line, however when looking at the histogram we see that

14
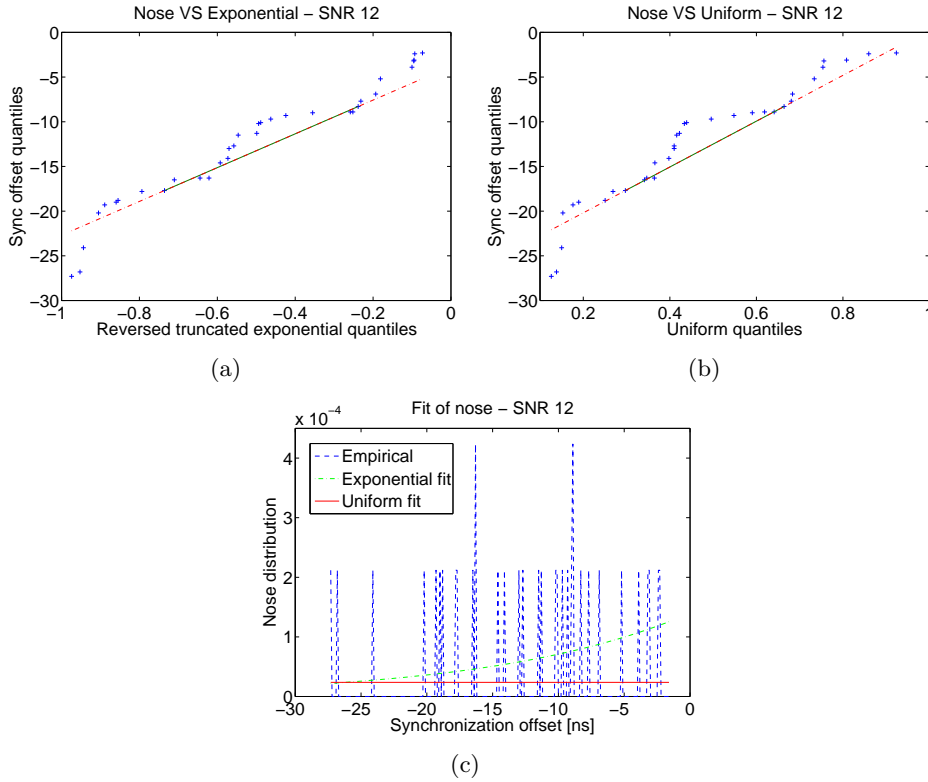
Figure 6: Fit of the nose of the distribution. (a) QQ plot against uniform distribution (b) QQ plot against truncated exponential distribution (c) Comparison of the shapes of the distributions.

there is only a few samples here and there. Therefore a uniform distribution might fit the nose as well as an exponential. This is confirmed by a QQ plot that shows little difference compared to the first one. In the end the uniform model is chosen because it is the simplest and :

$$f_{nose}(x) = \frac{1}{\alpha + 32}. \tag{22}$$

The peak as well looks difficult to handle. It is fairly flat on the top but decays quickly at the boundaries. In the QQ plot shown in Fig. 7, it seems to follow a truncated normal distribution, but when comparing to the histogram we can see that a normal distribution is too thin. It is too high at the center and too low on the sides, thus being overly optimistic. When

15
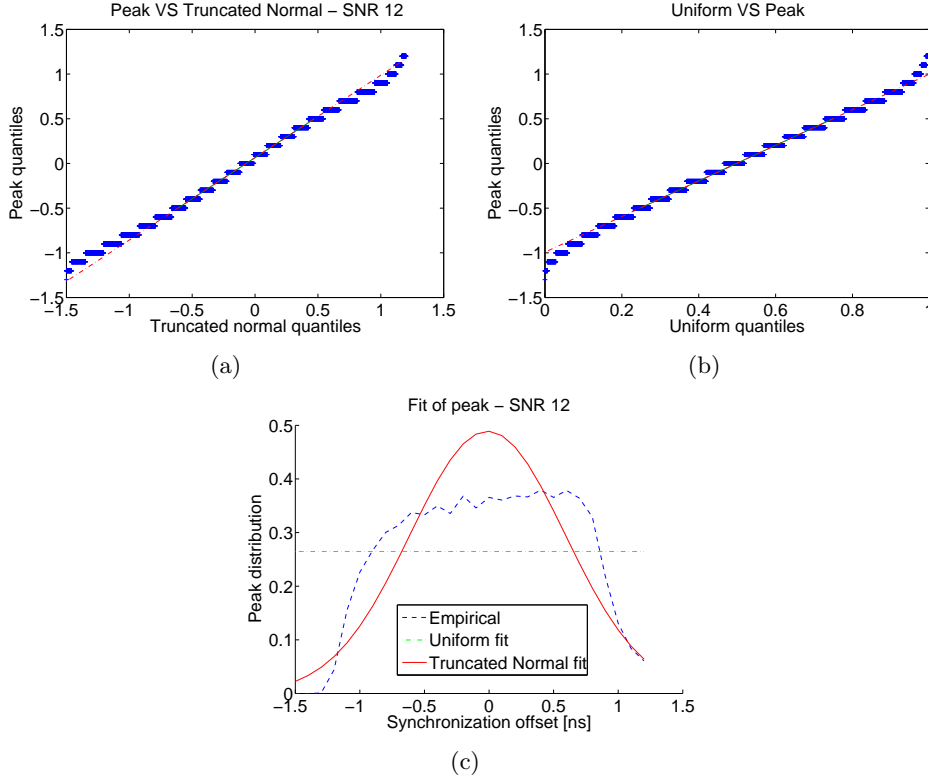
Figure 7: Fit of the peak of the distribution. (a) QQ plot against uniform distribution (b) QQ plot against truncated normal distribution (c) Comparison of the shapes of the distributions.

comparing to a uniform distribution, the QQ plot looks equally good but this time it is definitely too high at the boundaries while being too low at the center. In this case a uniform distribution is too pessimistic. Finally the Gaussian was chosen as it leads to a final model that is closer to a continuous distribution function. The mean μ and variance σ^2 are estimated as for a usual normal distribution :

$$\hat{\mu} = \frac{1}{|S_{peak}|} \sum_{x \in S_{peak}} x \tag{23}$$

$$\hat{\sigma}^2 = \frac{1}{|S_{peak}| - 1} \sum_{x \in S_{peak}} (x - \hat{\mu})^2 \tag{24}$$

16

and the probability distribution function is :

$$f_{peak}(x) = \frac{1}{\sqrt{2\pi}\hat{\sigma}} \frac{e^{-\frac{(x-\hat{\mu})^2}{2\hat{\sigma}^2}}}{\Phi\left(\frac{\beta-\hat{\mu}}{\hat{\sigma}}\right) - \Phi\left(\frac{\alpha-\hat{\mu}}{\hat{\sigma}}\right)}. \tag{25}$$

where $\Phi(x)$ is the cumulative distribution function of a zero-mean unit-variance normally distributed random variable.

Finally the tail seems to be quite heavy, therefore some heavy tail distribution seems appropriate. First a power law of the type $f(x) = ax^{-\tau}$ was tried. For this one we worked directly on the histogram. As $\log f(x) = \log a - \tau \log x$, the histogram should be linear in log-log space. To check this we take a histogram of the tail composed of K bins $B_1, \ldots, B_K$ corresponding to $x_1, \ldots, x_K$, remove the bins with no points inside ($B_k = 0$, because we need to take the logarithm). Then, we use a least-squares fit to a straight line on the pairs $(\log x_k; \log B_k)$, $B_k \neq 0$, to find $\log a$ and τ. However, the result was not successful, as shown in Fig. 8.

Then, an exponential distribution was tried. Already the QQ plot shows almost a straight line. This seems therefore a good model for the tail. The parameter of the exponential is then calculated as :

$$\hat{\lambda} = \frac{|S_{tail}|}{\sum\limits_{x \in S_{tail}} x} \tag{26}$$

and the pdf is :

$$f_{tail}(x) = \hat{\lambda} e^{-\hat{\lambda}(x-\beta)} \tag{27}$$

The final result is shown in Fig. 9. The boundaries between the three parts were chosen manually to be $\alpha = -1.5$ ns and $\beta = 1.2$ ns. Then the evolution of $\hat{\mu}$, $\hat{\sigma}$ and $\hat{\lambda}$ as a function of the SNR is shown in Fig. 11. A 2D histogram for different SNR is also shown along with the evolution p_{nose}, p_{peak} and p_{tail}, the weights of the different parts of the distribution, in Fig. 10. It can be observed that the length of the tail is maximum for some intermediate value of the SNR (around dB). When the SNR is very low, it seems there is a binary behavior, either synchronization succeeds with good precision either it fails completely. When the SNR is high the precision also gets better. However the tail remains very heavy, with offset up to 20 ns (6 m) with relatively high probability. At 25 dB, the probability to be in the tail is still around 10%.
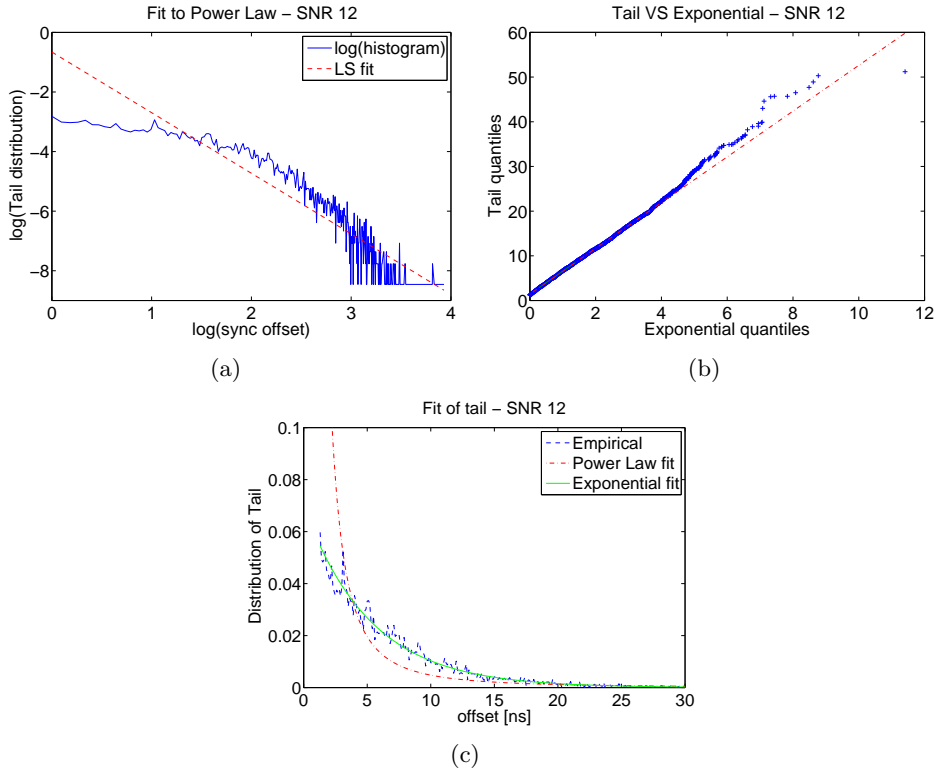
Figure 8: Fit of the tail of the distribution. (a) Fit to a power law (log-log) (b) QQ plot against exponential distribution (c) Comparison of the shapes of the distributions.

2.3 With Multiple User Interference

The simulations were redone with an interferer ten times stronger than the user of interest. No modelling has been done yet, but a 2D histogram again along with the evolution of p_{nose}, p_{peak} and p_{tail} is shown in Fig. 13. We can observe in Fig. 12 that there is significant weight in the nose this time due to the back search algorithm especially at high SNR. When the SNR goes close to zero, we fall back in a pattern similar to the single user case.
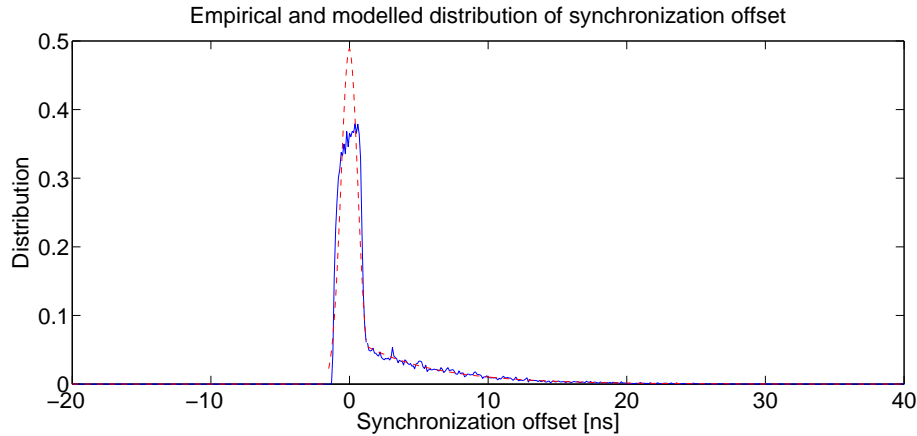
Figure 9: Fit of the tail of the distribution. (a) Fit to a power law (log-log) (b) QQ plot against exponential distribution (c) Comparison of the shapes of the distributions.

3 Conclusion

In section 1 the state-of-the-art in localization was revised. As for the measurement technique, the only appropriate method for wireless sensor networks without good clock synchronization is two-way TOA measurements. However, it requires a lot of redundancy when actually taking the measures in a network. In order to mitigate this there is two possible orientation :

- Try to use the properties of UWB communication to find an efficient scheme.

- Use a scheme based on differential TDOA (dTDOA) as described in [4] could also be studied as it doesn't require clock synchronization and also mitigate the error due to clock drifts.

It was also shown that neither Least-Squares nor Gaussian based Maximum Likelihood estimation give a performance sufficient for acceptable precision when the measurement noise is not Gaussian. There is therefore a need for better algorithm on the one hand and to reduce to the minimum the measurement error on the other hand.

In section section 2, the synchronization error was analyzed and indeed found to be highly non-Gaussian. It is heavy-tailed with a tail that doesn't shrink so much as the SNR becomes higher. The central part of the distribution could not be fit very well and will require some more effort to be

19
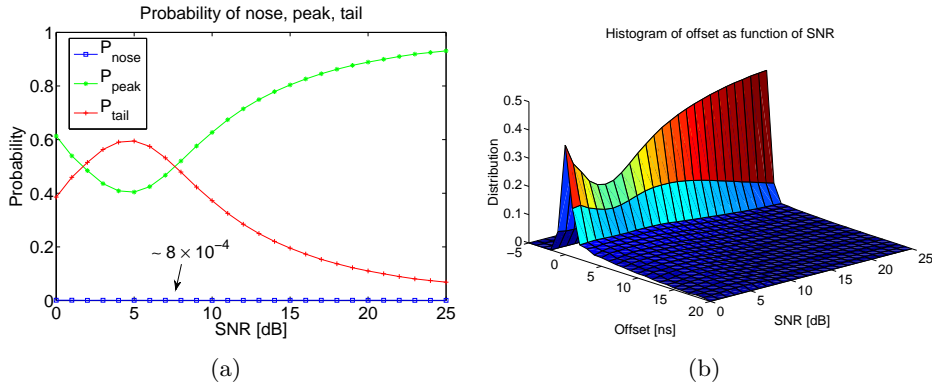
Figure 10: The length of the tail is maximum at about 5 dB. At this SNR, the probability to be in the tail is about 0.6. However, the probability to be in the nose is almost zero. (a) Evolution of p_{nose}, p_{peak} and p_{tail} with the SNR (b) The histograms of the synchronization offset as a function of the SNR.

realistic. Also, the distribution found needs more validation. To begin with, the model could be used to generate samples that would be compared to the output of the simulator. Secondly, a goodness of fit, or some other statistical tests could be performed to assess the model.

Also, it should be noted that the simulation environment was not optimized at all for ranging. There is therefore plenty of room for optimization. For example, a pre-defined payload could be used to enhance the synchronization.

3.1 Future work

- The synchronization error should be analyzed more in details for the Multiple User Interference case.

- An efficient distributed measurement algorithm should be investigated, taking into accounts the properties of UWB.

- There is the possibilities to derive a better Maximum Likelihood Estimator based on the findings of 2.

- Another possibility is to optimize the synchronization algorithm to reduce the error.
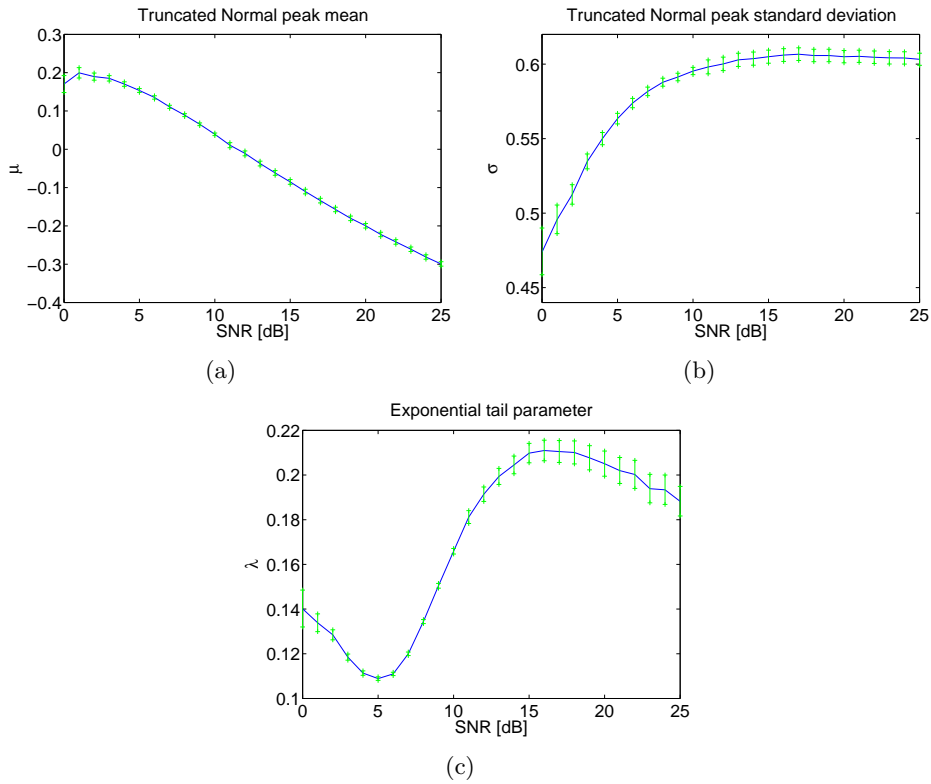
Figure 11: The evolution of the parameters of the fit as a function of the SNR. (a) Mean of truncated normal (b) Standard deviation of truncated normal (c) Parameter of the exponential tail.

- Then, a distributed version of the localization algorithm should be developed.

- Finally the complete distributed localization algorithm should be simulated to determine its performance in realistic conditions.

Thanks

To Ruben Merz for his enthusiastic supervision even close to his final thesis submission and to Manuel Flury for his precious help and advice with the simulator.
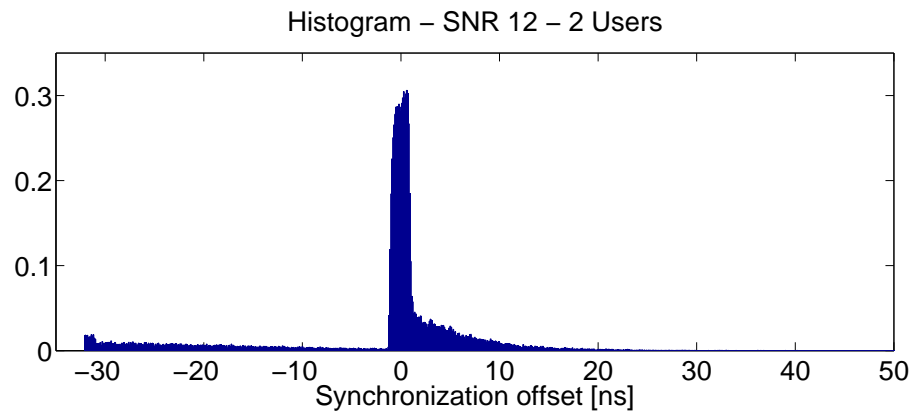
Figure 12: The histogram of the synchronization offset at an SNR of 12 dB when an interferer is present.

References

[1] N. Patwari, J. N. Ash, S. Kyperountas, A. O. Hero III, R. L. Moses, and N. S. Correal, "Locating the Nodes : Cooperative localization in wireless sensor networks," *Signal Processing Magazine, IEEE*, vol. 22, pp. 54–69, July 2005.

[2] A. Sayed, A. Tarighat, and N. Khajehnouri, "Network-based wireless location: challenges faced in developing techniques for accurate wireless location information," *Signal Processing Magazine, IEEE*, vol. 22, pp. 24–40, July 2005.

[3] F. Gustafsson and F. Gunnarsson, "Mobile positioning using wireless networks: possibilities and fundamental limitations based on available wireless network measurements," *Signal Processing Magazine, IEEE*, vol. 22, pp. 41–53, July 2005.

[4] H. Fan and C. Yan, "Asynchronous Differential TDOA for Sensor Self-Localization," *Acoustics, Speech and Signal Processing, 2007. ICASSP 2007. IEEE International Conference on*, vol. 2, pp. II–1109–II–1112, April 2007.

[5] F. Sivrikaya and B. Yener, "Time synchronization in sensor networks: a survey," *Network, IEEE*, vol. 18, pp. 45–50, July-Aug. 2004.
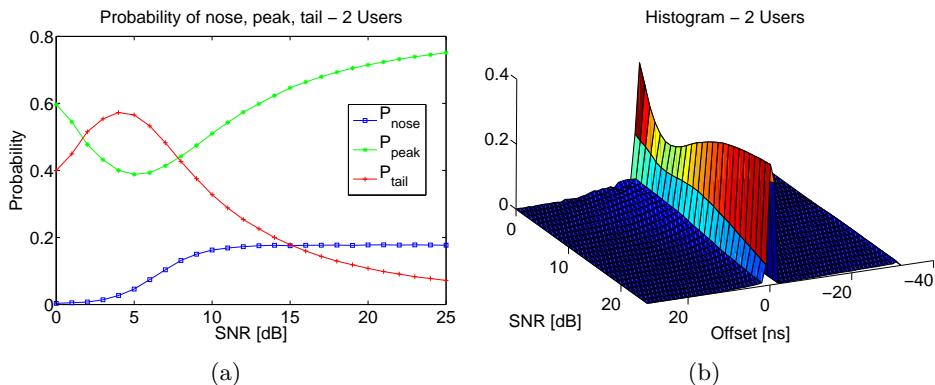
Figure 13: The length of the tail is maximum at about 5 dB. At this SNR, the probability to be in the tail is about 0.6. However when Multiple User Interference is present, the weight of the tail increases with the SNR. (a) Evolution of p_{nose}, p_{peak} and p_{tail} with the SNR (b) The histograms of the synchronization offset as a function of the SNR.

[6] B. Fang, "Simple solutions for hyperbolic and related position fixes," *Aerospace and Electronic Systems, IEEE Transactions on*, vol. 26, pp. 748–753, Sep 1990.

[7] J. Caffery Jr., "A new approach to the geometry of TOA location," *Vehicular Technology Conference, 2000. IEEE VTS-Fall VTC 2000. 52nd*, vol. 4, pp. 1943–1949, 2000.

[8] J. Abel, "A divide and conquer approach to least-squares estimation," *Aerospace and Electronic Systems, IEEE Transactions on*, vol. 26, pp. 423–427, Mar 1990.

[9] Y.-T. Chan, H. Y. C. Hang, and P.-C. Ching, "Exact and Approximate Maximum Likelihood Localization Algorithms," *IEEE Transactions on Vehicular Technology*, vol. 55, pp. 10–16, January 2006.

[10] N. B. Priyantha, H. Balakrishnan, E. Demaine, and S. Teller, "Anchor-Free Distributed Localization in Sensor Networks." LCS Tech. Report #892, April 2003.

[11] D. Moore, J. Leonard, D. Rus, and S. Teller, "Robust distributed network localization with noisy range measurements," in *Proceedings of*

the Second ACM Conference on Embedded Networked Sensor Systems (SenSys '04), Baltimore, MD, pp. 50–61, November 2004.

A Network-wide Localization Algorithms

We considered in section 1 a case where we know perfectly the coordinates of a set of reference nodes and we want to localize some target node. However, in a practical sensor network there is no such reference nodes. Even if some nodes are relatively static and can get a good estimate of their position, there will still be some error in those estimates. A GPS receiver is too costly and manual configuration too cumbersome for practical, large, sensor notworks. In addition, there might also be no static nodes at all. Therefore, the positions of all nodes in the network must be estimated together.

A.1 Mass-spring Optimization

The standard solution to this problem is solving a global mass-spring optimization problem. This is a reference to the physical problem of finding the equilibrium, or minimum-energy configuration, of a system composed of masses connected together by springs. Here the masses and the springs corresponds respectively to the nodes and the distances between the nodes. First, the nodes are initialized to some positions, then the positions of the nodes are changed by small steps until a minimum energy configuration is reached. This corresponds to the minimization of a global error function given by :

$$E = \sum_i (r_i - \hat{r}_i)^2 \tag{28}$$

where i is an index covering all the edges in the graph of the network, r_i is the true length of the edge and $\hat{r}_i$ is its estimate.

There are however some problems to this approach. First, the risk of convergence to local minimum is high. In addition to this, it might happen that the true graph is also itself a local minima of the error function. This is mostly due to ambiguities in the graph due to a low connectivity of the nodes. To solve this problem, [10] proposes an initialization algorithm which leads to good solutions of the problem. It sets the nodes the furthest apart at the edge of the graph and use them as reference for the rest of the nodes in an attempt to have an initialization close to the true graph. On the other hand, [11] separates the network into sub-graphs where the node degree is at least three. Then the sub-graphs are rigid and there are no ambiguities in the nodes positions. It also excludes isolated nodes.